Surface electromagnetic waves with damping. I. Isotropic media*

G. S. Kovener,† R. W. Alexander, Jr., and R. J. Bell
Graduate Center for Materials Research and Physics Department, University of Missouri-Rolla, Rolla, Missouri 65401
(Received 2 February 1976)

Surface-electromagnetic-wave dispersion curves are usually calculated using a simple equation derived from Maxwell's equations and boundary conditions. When complex dielectric functions are used for the two media, the component of the propagation vector along the surface, k_x, becomes infinite as the frequency approaches the surface polariton frequency ω_s if ω is considered complex and k_x is real. On the other hand, if k_x is considered complex and ω real, the dispersion curves bend back toward smaller k_x as ω approaches ω_s. We have previously demonstrated that both types of behavior can be obtained from attenuated-total-reflection measurements of silver. We now extend this result to other materials and show that dispersion curves alone present an inadequate summary of the data.

I. INTRODUCTION

There has been considerable discussion of the dispersion curves of surface electromagnetic waves (SEW) when absorption is included.[1-14] Without absorption, that is, with the imaginary part of the dielectric function $\epsilon_2(\omega)$ neglected, the dispersion curves show k_{1x} becoming infinite at the surface wave frequency, ω_s. The surface wave frequency satisfies $\epsilon_1(\omega_s) = -1$, where $\epsilon_1(\omega)$ is the real part of the complex dielectric function $\epsilon(\omega) = \epsilon_1(\omega) + i\epsilon_2(\omega)$. The real part of the component of the propagation vector parallel to the surface is k_{1x}. If $\epsilon_2(\omega) \neq 0$, then a plot of ω versus k_{1x} does not have a singularity at ω_s and the dispersion curve bends back toward smaller k_{1x} as ω_s is approached. In his early measurements of the SEW dispersion curve on silver using attenuated total reflection (ATR), Otto[2] found the experimental dispersion curve did not bend back. However, Arakawa, Williams, Hamm, and Ritchie[7] found that the SEW dispersion curve for silver did bend back. They also had used ATR to measure the dispersion curve. The purpose of this paper is to show that both ATR measurements can be understood using the usual Fresnel equations[15] so that the two differing results are not contradictory.[1]

We begin Sec. II by reviewing the theory to establish our notation and then show the utility of presenting the calculations for the ATR reflectivity in terms of a surface in a three-dimensional space. The experimental results are then discussed in terms of this ATR surface and shown to be consistent with each other. Section III demonstrates the general utility of the ATR surface for understanding experimental results. The effects of finite beam divergence are also considered. Finally in Sec. IV we briefly discuss the problem of relating the experimental results to calculated dispersion curves and indicate that an interesting problem remains to be solved.

II. DISPERSION CURVES WITH DAMPING

Dispersion curves for elementary excitations are usually treated in the absence of damping, and inclusion of damping considerably complicates the situation.[1-4] This has been pointed out for bulk excitations in a review article by Barker and Loudon. Much of the discussion has been in the context of Raman scattering. In this paper we shall restrict ourselves to surface electromagnetic waves on isotropic media and postpone a discussion of anisotropic media.[14] We show that there is an ambiguity in what is meant by the dispersion curves when damping is present, and further that care must be exercised in relating the minima in reflectivity observed using ATR techniques to the dispersion curves.

To simplify our discussion, we shall consider SEW on an infinite half space, $z < 0$, with the $z > 0$ half space being vacuum. Then the dispersion curves for SEW are the solutions to[2,5]

$$k_x = (\omega/c)\{\epsilon(\omega)/[\epsilon(\omega)+1]\}^{1/2}, \tag{1}$$

where $\epsilon(\omega) = \epsilon_1(\omega) + i\epsilon_2(\omega)$ is the dielectric function of the medium and k_x is the component of the propagation vector along the surface. Usually $\epsilon_2(\omega)$ is considered to vanish, and then k_x is purely real for those frequencies for which SEW exist, i.e., those frequencies for which $\epsilon_1(\omega) < -1$. In the absence of damping, $k_x \to \infty$ at the surface wave frequency ω_s where $\epsilon_1(\omega_s) = -1$.

In the presence of damping, $\epsilon_2(\omega) \neq 0$, Eq. (1) becomes complex and if ω is chosen to be real, then k_x is complex. The real part of k_x describes the propagation wave vector and the imaginary part of k_x describes the spatial damping in a manner frequently encountered in optics.[14] The real

part k_{1x} of k_x is used to plot the dispersion curve. In this case, however, the dispersion curves bend back toward smaller k_{1x} as ω approaches ω_s, rather than k_{1x} becoming infinite at this frequency.[5] This difference in behavior is illustrated in Fig. 1, where the dielectric function for silver[16] has been used. The dashed line is for $\epsilon_2 = 0$ and the solid line for $\epsilon_2 \neq 0$. For the moment, ignore the curves above ω_s.

Now consider what is measured in an ATR experiment. Two slightly differing methods have been employed. Otto measured the ATR reflectivity with the angle of incidence fixed and incident photon energy varied.[2] Arakawa and co-workers,[7] on the other hand, fixed the incident photon frequency and varied the angle of incidence θ. In either case, the minimum in the reflectivity is associated with excitation of the surface electromagnetic wave, and k_{1x} is found from the momentum conservation equation

$$k_{1x} = (\omega_{\min}/c) n_p \sin\theta_{\min} . \tag{2}$$

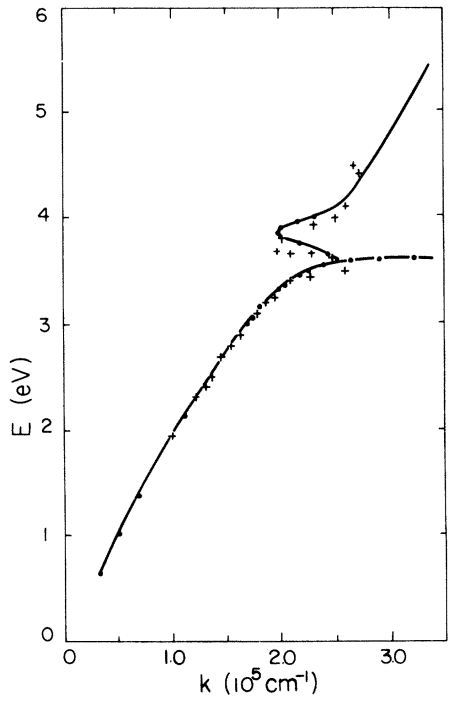

FIG. 1. Dispersion curves for a 340-Å silver film on a CaF_2 prism. Solid curve, obtained from cross section of the ATR reflectance surface for fixed frequencies. This solid curve also results from solving Eq. (1) using complex k_x and $\epsilon(\omega)$. Dash-dot line, from cross sections for fixed angle. This dash-dot curve also results from solving Eq. (1) with $\epsilon(\omega)$ purely real or with ω complex and k real. Crosses are experimental points of Arakawa *et al.* (Ref. 7) who fixed the frequency and varied the angle.

The prism refractive index is n_p, and for the moment, we assume the gap between the prism and the sample is sufficiently large that the effect of the prism on the surface electromagnetic waves is negligible. The incident photon frequency and angle of incidence at the reflectivity minimum are $\omega_{\min}$ and $\theta_{\min}$. It has been found that the dispersion curves [a plot of $\omega_{\min}$ vs k_{1x} from Eq. (2)] are not the same for the two methods of measurement. In Fig. 1 are plotted the dispersion curves for silver-air measured by Otto using the first method and by Arakawa *et al.* using the second method. Note that in these experiments, the silver film itself served as the gap between the prism and the silver-air interface as shown in the inset of Fig. 1. Otto's measured dispersion curve has no bend back, while Arakawa's does show bend back. And in fact, Otto's measurements agree with the dispersion curve calculated neglecting damping, while Arakawa's data agree with the curve calculated with $\epsilon_2 \neq 0$. The curves in Fig. 1 were calculated using the optical constants from Johnson and Christy.[16]

How is this apparent contradiction to be resolved? We will now show that both measurements are in agreement with Fresnel's equations. However, we are unable to demonstrate why Otto's method yields dispersion curves agreeing with those calculated with $\epsilon_2 = 0$, while Arakawa's method produces curves agreeing with those calculated with $\epsilon_2 \neq 0$.

To show that the two measurements discussed above are in reality consistent with each other, the ATR reflectivity was calculated as a function of both the incident photon energy and the angle of incidence. Fresnel's equations for a layered system as given by Wolter[17] were used with the experimental geometry as shown in the inset of Fig. 2. No correction was applied for reflection at the prism entrance and exit faces. The refractive index of the CaF_2 prism was 1.434 and the film was 340 Å thick. The range of ω was 3.0–4.25 eV, with the range of incident angles from 45° to 75°. The optical constants of the silver film were taken from Johnson and Christy.[16]

Plotting the calculated reflectivity as a function of both incident photon energy and angle of incidence gives the surface shown in Fig. 2. There are two valleys in this reflectance surface. The lower energy valley is due to surface plasmons, while the other valley is due to a bulk plasmon $[\epsilon_1(\omega) = 0]$. If the experiment is done by fixing the angle and scanning the frequency, the ATR spectrum is a cross-section line going from left to right. Alternatively, if the frequency is fixed and the angle scanned, the ATR spectrum is a cross-section line going from bottom to top. Some representa-

tive cross sections are shown in Figs. 3(a) and 3(b). The frequencies of successive cross-section minima are converted to momenta using the ATR equation [Eq. (2)] and then plotted in Fig. 1. The dashed line is the result obtained for fixed angle cross sections and the solid line for fixed frequency cross sections. It is evident that the dashed curve approaches an asymptote while the solid line bends back. The crosses are the data points of Arakawa *et al.*, and the slight discrepancy near 3.7 eV is due to sample differences between Johnson and Christy and Arakawa *et al.* In this region, the real part of $\epsilon(\omega)$ approaches -1, and the ATR reflectivity minima are sensitive to small variations in $\epsilon(\omega)$.

The reason for the bend back using fixed frequencies can be seen qualitatively by a careful examination of the reflectance surface. As one selects successive fixed energy cross sections, the spectra obtained become more and more parallel to the axis of the SEW valley near 3.7 eV. When the energy is sufficiently large, the spectra are no longer located in the minimum of this valley but climb the ridge between the surface plasmon and bulk plasmon valleys. The curves of Fig. 3(b) clearly illustrate this anomalous behavior. The dispersion curve measured by Otto for silver agrees with the calculated dash-dot line of Fig. 1.

Thus, the same set of optical constants, with Fresnel's equations, predict both Otto's results obtained by varying the incident photon frequency with angle of incidence fixed, and Arakawa's results obtained by fixing incident frequency and varying θ. This consistency is obtained despite the large differences in the "dispersion curves" plotted by the two investigators.

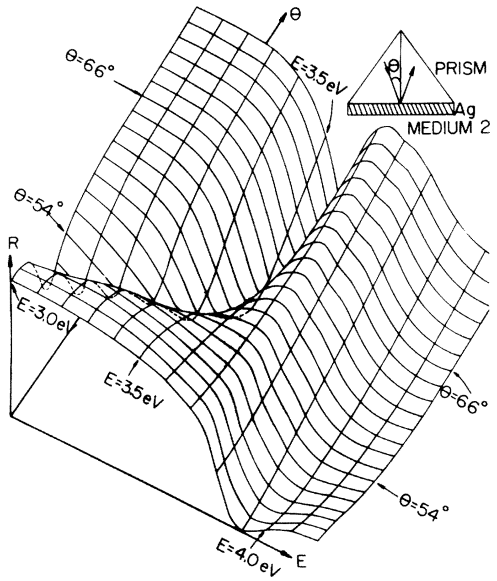

FIG. 2. The ATR reflectance of a 340-Å-thick Ag film on a CaF_2 prism plotted as a function of the incident frequency ω and the angle of incidence θ. Inset, ATR geometry of a prism or semicylinder (index of refraction n_p) with a silver film and a second interface with another medium.

III. APPLICATIONS

The reflectance surface is an ideal way of easily visualizing the influence of the gap spacing in those ATR measurements with an air gap between the sample and prism. The gap spacing is an important factor in determining the features of the spectra since there are two fields exponentially decaying across the gap. One field due to the incident light has its maximum at the prism-gap interface. The other evanescent field is due to the SEW and has its maximum value at the gap-absorber interface. For small gaps, the SEW may recouple back into the prism, but the effect of gap spacing is also influenced by the value of ω and k_x. An expression for the optimum gap spacing has been derived by Otto[18,19] with some approxima-

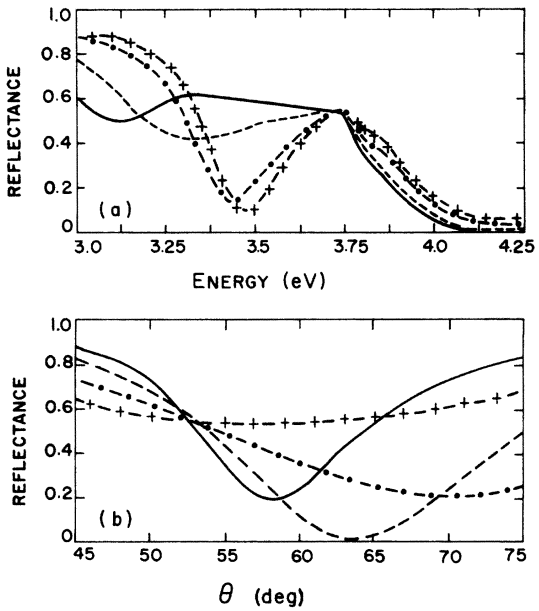

FIG. 3. (a) Cross sections of the ATR reflectance surface of Fig. 2 obtained by holding the angle of incidence fixed and varying the incident frequency. The solid line is $\theta = 52°$, dashed is $\theta = 54°$, dashed-dot is $\theta = 58°$, and dash-hatch is $\theta = 60°$. (b) Cross sections of the ATR reflectance surface of Fig. 2 obtained by holding the incident frequency fixed and varying θ. The solid line is incident frequency of 3.4 eV and the dash-hatch line is 3.7 eV. Note how the minimum in Fig. 3(a) moves toward higher frequencies as θ increases, while the last minimum moves back towards smaller θ (and hence smaller k_{1x}).

TABLE I. NaCl oscillator parameters.

ω_i (cm^{-1})	$\delta\epsilon_i$	Γ_i (cm^{-1})
164	3.1975	6.13
247	0.0898	34.7
	$\epsilon_\infty = 2.32$	

tions, but because the reflectance surface displays the response for a wide range of ω and θ, it is a more effective aid for looking at this gap dependence.

NaCl was chosen for this investigation since it has been examined experimentally by Bryksin *et al.*[20] In this case, the NaCl sample was separated from the base of the prism by various air gap spacings. The calculations were done for frequencies from 150 to 250 cm^{-1} and incident angles from 20° to 60° in the prism (silicon, $n_p = 3.418$). The reflectance surfaces were generated for several air gap spacings: 12, 5, and 2 μm. The NaCl dielectric function was calculated from the oscillator model and the parameters of Bryksin *et al.*[20] (Table I). The phonon damping was not frequency dependent.

Figure 4 shows the reflectance surface with a gap spacing of 5.0 μm. The "valley" of Fig. 5 clearly "turns" toward smaller frequencies as θ is decreased. Note the sharp rise in reflectivity of the SEW minima near the critical angle (17° for a silicon prism).

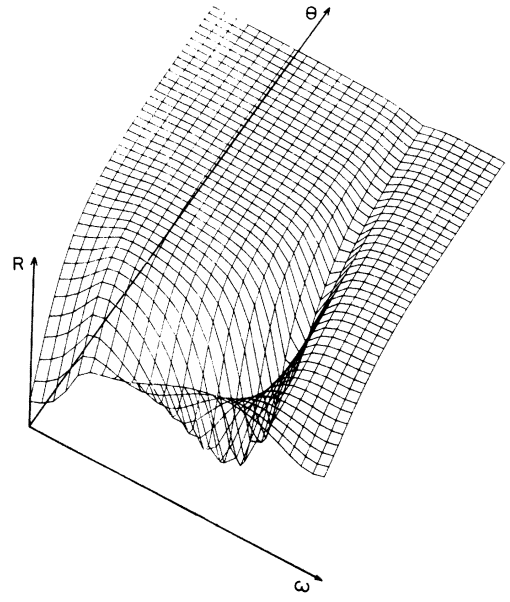

FIG. 4. ATR reflectance surface of NaCl with a 5.0 μm air gap spacing. The frequencies along the lower axis are 150–250 cm^{-1}. The incident angles along the upper axis are 20° to 60°.

The dispersion curves resulting from the minima are shown in Fig. 5. (To compute these minima a smaller grid was used than that of Fig. 4.) The solid curves B and C are obtained from minima with frequency fixed; dashed curves B and C are obtained with incident angle fixed. Curve B is with a 5.0 μm gap and curve C with a 2.0 μm gap. The triangles correspond to a gap of 12.0 μm and for clarity are not connected with a smooth curve. The crosses are the experimental points obtained from Bryksin *et al.*[20] The value of the gap spacing they used is not given, but we estimate from the reflectance spectra given in their article that $d \sim 10$–11 μm. The solid line A is obtained from Eq. (1) with $\mathrm{Im}[\epsilon(\omega)] = 0$ and the dashed line A using a complex $\epsilon(\omega)$ and the real part of k_x.

The reflectance minima curve approaches the calculated dispersion curve Eq. (1) at small k only for large gap spacings. This is expected since the SEW will strongly couple back to the prism via the evanescent field of the SEW at small

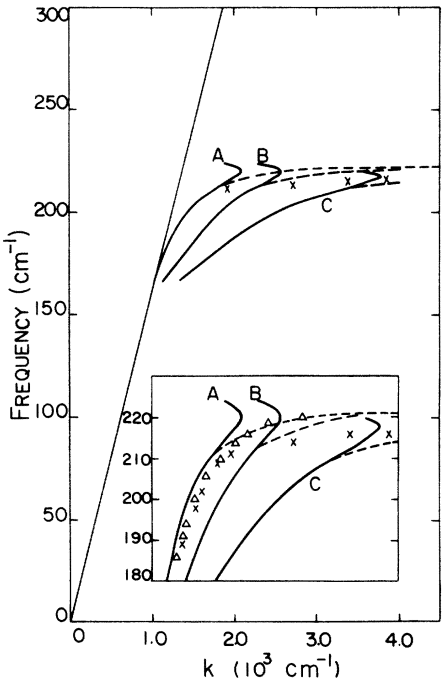

FIG. 5. Dispersion curves of NaCl obtained from the ATR reflectance surface minima. The inset is a detailed view. The solid lines B and C are plotted from the cross sections with frequency fixed; the dashed curves B and C are plotted from cross sections with incident angle fixed. Curve B is from the reflectance surface of Fig. 5 with a 5.0 μm gap spacing. The triangles correspond to a 12.0 μm gap. Curve A is the dispersion relation Eq. (1) with $\epsilon(\omega)$ complex (solid line) and $\epsilon(\omega)$ purely real (dashed line). The crosses are experimental points of Bryksin *et al.*[2] The straight line is the free space photon dispersion line.

gaps. Indefinitely large gaps cannot be used since the reflectivity minimum is substantially reduced at larger angles for large gaps.[21] However, for all gap spacings, the fixed angle minima (dashed curves) approach the asymptote of Eq. (1) for sufficiently large k, but the experimental data appear to approach an asymptote of lower frequency, as noted by Bryksin. We attempted to improve the fit by considering a finite beam as discussed in the next section, but no appreciable change was noted in the reflectance minima curves.

It is therefore certain that the discrepancy in frequencies is not due to recoupling across the gap or finite beam divergence. Because the purpose of this paper is to demonstrate the reflectance surface technique, we have not attempted different damping parameters or frequency dependent damping parameters in an attempt to reconcile the difference. The ability of the reflectance surfaces to easily represent all facets of the gap spacing is obvious.

The full width half-maximum (FWHM) of the ATR spectra is of interest because it is an indication of the damping of the SEW and thereby the absorbing material. We have found that a straightforward measurement of FWHM and its conversion to the material damping parameter does not include all the parameters which determine the FWHM. One can decide from an examination of the reflectance surface that the FWHM is also controlled by the gap spacing and the incident angle in a manner that is difficult to perceive with other analytical techniques. That is, the ATR cross sections measured do not cross the valleys at right angles, and this increases the observed width of the spectra. Once again, we will select an example to demonstrate this.

InSb has been studied extensively using the grating technique[22,23] and the ATR technique.[24,25] Although no appreciable difference is apparent between calculated and measured SEW dispersion curves, the ATR linewidth of the upper branch is larger by two to three times the width expected from the bulk electronic damping constant τ. We will include the finite beam divergence using an integrated spectra approach in an attempt to reduce this linewidth discrepancy.

The free-carrier concentration in InSb produces strong plasmon-phonon coupling for electron concentrations on the order of 10^{17} cm^{-3}. In addition, the conduction band is nonparabolic, so the effective mass m^* is a function of the concentration.[26] For a carrier concentration of 2.0×10^{17} cm^{-3} there are two frequency regions for SEW: one below ω_{T0} and one between ω_{T0} and ω_p. The InSb parameters used to calculate the dielectric function are given in Table II.

TABLE II. InSb oscillator parameters.

ω_t (cm^{-1})	179	N (cm^{-3})	2.00×10^{17}
$\delta\epsilon$	2.0	m^*	0.022 m_e
Γ (cm^{-1})	2.864	τ (cm^{-1})	10.0
ϵ_∞	15.7		

A fixed angle cross section for $\theta = 22°$ is detailed in Fig. 6. The crosses in Fig. 6 are the experimental data of Bryksin *et al.*[25] One must be very careful in relating the FWHM of the ATR spectra to the damping of the SEW. The shape of the minima is determined by the ATR parameters of θ and gap spacing d as well as the material parameters. The influence of θ and d on the width is clearly apparent in the Figs. 5 and 6 for NaCl. Therefore if one desires to measure the material damping using SEW, the experimental variables θ and d must be accurately measured and d should be uniform.

The finite divergence of the incident beam is considered by integrating at a fixed frequency over a range of incident angles centered about θ_0. The reflectivity is weighted with a Gaussian of standard deviation of one degree; the angular integration interval included 99.4% of the incident beam. The result of this treatment is displayed in Fig. 6. The solid curves are the spectra obtained by the integration method. The two curves A are calculated with a gap spacing of 19 μm and the two curves B with a gap spacing of 8 μm. As one can see, the minimum after integration moves toward lower frequencies for the 19 μm gap (A) but toward higher frequencies for the 8 μm gap (B). The shift between A and B is due to the effect of the gap as discussed earlier for NaCl. For

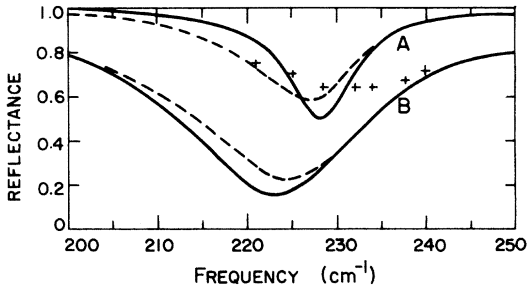

FIG. 6. ATR spectra with a divergent incident beam. The solid curves are spectra calculated without the angular integration and the dashed curves are the spectra after the integration treatment. The A curves are spectra with a 19 μm gap spacing and the B curves with a 8.0 μm gap spacing. Note the different directions of the shift in the dashed-curve minimum relative to the solid curve for A and B. The crosses are the experimental points of Bryksin *et al.*[2]

measurements at smaller angles where the dispersion curve is near the light line, the minimum shift is reduced, but the amount of change is difficult to predict without this integration. Any attempt to include a nonuniform gap spacing would require a finite width beam treatment of the ATR technique, which we did not attempt.[27] This underscores the requirement that the experimental conditions be rigidly controlled in order to plot dispersion curves from the ATR spectra.

IV. DISCUSSION

Dispersion curves are usually discussed in the context of no damping. For surface electromagnetic waves this gives the usual dispersion curve with k_x (which is real) becoming infinite at ω_s, where $\epsilon(\omega_s) = -1$. Although most discussions have neglected to mention it, for surface phonons, k_x becomes infinite also at the lower frequency, where $\epsilon(\omega) = -1$ also. This is obvious from Eq. (1). When damping is included so that $\epsilon(\omega)$ is complex, then one must make either ω or k_x complex. If ω is chosen as complex, with k_x real, it is generally impossible to find an analytical expression for the dispersion curve [i.e., an analytic expression for $\mathrm{Re}(\omega)$ as a function of k]. However, a solution has been found numerically for InSb by Gammon and Palik,[9] who find the resulting dispersion curve to be very close to that obtained using real $\epsilon(\omega)$. This is, no bend back occurs, and k_x becomes large as ω approaches ω_s. If, however, we take k_x complex and ω real, then the imaginary part of the denominator of Eq. (1) never vanishes, so the real part of k_x never becomes infinite, and the dispersion curve (k_{1x} vs ω) exhibits bend back near ω_s, as seen in Fig. 1. It is not obvious that the dispersion curve obtained in this manner should agree with that obtained by taking cross sections of the ATR surface at fixed photon frequencies, although such agreement is found.

A similar problem for bulk polaritons within the context of Raman scattering[8-12,14] has been discussed in the literature. Several authors[9-12,28] have used a temporal damping (ω complex) treatment for bulk polaritons which have the usual dispersion relation

$$k = (\omega/c)\sqrt{\epsilon}\,. \tag{3}$$

The real ω roots of the polynomial do not exhibit bend back as k_x increases, but the roots asymptotically approach a limiting frequency. However, Giallorenzi[12] points out that the solution does not differ substantially from that obtained by taking only the real part of $\epsilon(\omega)$, just as for SEW.

Puthoff *et al.*[13] have made the calculation keeping ω real and found the dispersion curves also bend back in a manner similar to that found for SEW dispersion curves with k_x complex.

Another way to understand this difficulty with the dispersion curves is to consider it as an attempt to describe the normal modes of a system that has damping. If one considers the excitation as a wave propagating along a surface, then spatial damping (complex k_x) is appropriate. Conversely viewed as an excitation of a normal mode that decays in time, temporal damping (complex ω) is required.

The way to avoid these difficulties is to consider the quantities measured in the experiment. As we have shown, the ATR surface resolves the differences between the two experimentally determined dispersion curves.

V. CONCLUSION

The ATR surface has been used to show how dispersion curves for surface electromagnetic waves with or without bend back can be obtained from measurements of ATR spectra. Theoretically, no bend back occurs if the dielectric function is purely real. The introduction of an imaginary part of the dielectric function complicates the picture because the poles now occur for complex values of k and ω. If one mades k_x real and ω complex, bend back does not occur, while complex k_x and real ω produces bend back in the dispersion curves. The ATR reflectivity surface then shows the relation between the two experimental conditions: fixed θ, variable ω and fixed ω, variable θ. The first produces minima curves which do not bend back, while the second condition produces curves which do bend back. Also, the problem of defining what is meant by an SEW becomes difficult because the decay of the fields away from the surface into the medium is always exponentially damped.[29-31] In fact, dips may appear in the ATR spectrum where there is no SEW, at least according to the usual criterion found without damping. This will be illustrated in a future paper.[14]

In addition, the qualitative effect of a divergent incident beam can be visualized by considering the shape of the minima in the surface. A quantitative example is given for InSb with two gap spacings, and the shift in the upper branch minimum is shown to be toward higher frequency for one gap spacing and toward lower frequencies for another.

The application of the reflectance surface technique is not limited to isotropic materials, and we will publish theoretical and experimental results for MnF_2 in a forthcoming paper.[14]

ACKNOWLEDGMENTS

We would like to thank C. A. Ward for her programming. One of us (RWA) acknowledges the support of the Research Corporation.

---

*Research done under the Air Force Office of Scientific Research (AFOSR-76-2938) and the NSF (DMR74-19153).

†Present address: Amoco Chemical Corp., P. O. Box 400, Naperville, Ill., 60540.

[1]R. W. Alexander, G. S. Kovener, and R. J. Bell, Phys. Rev. Lett. 32, 154 (1974).

[2]A. Otto, Z. Phys. 216, 398 (1968).

[3]R. H. Ritchie, Surf. Sci. 34, 1 (1973).

[4]K. W. Chiu and J. J. Quinn, Nuovo Cimento B 10, 1 (1972).

[5]R. J. Bell, R. W. Alexander, Jr., W. F. Parks, and G. Kovener, Opt. Commun. 8, 147 (1973).

[6]R. W. Gammon and E. D. Palik, J. Opt. Soc. Am. 64, 350 (1974).

[7]E. T. Arakawa, M. W. Williams, R. N. Hamm, and R. H. Ritchie, Phys. Rev. Lett. 31, 1127 (1973).

[8]A. S. Barker, Jr. and R. Loudon, Rev. Mod. Phys. 44, 18 (1972).

[9]H. J. Benson and D. L. Mills, Phys. Rev. B 1, 4835 (1970).

[10]R. R. Alfano, J. Opt. Soc. Am. 60, 66 (1970).

[11]R. R. Alfano and T. G. Giallorenzi, Opt. Commun. 4, 271 (1971).

[12]T. G. Giallorenzi, Phys. Rev. B 5, 2314 (1972).

[13]H. E. Puthoff, R. H. Pantell, B. G. Huth, and M. A. Chacon, J. Appl. Phys. 39, 2144 (1968).

[14]G. S. Kovener, R. W. Alexander, Jr., and R. J. Bell (unpublished).

[15]M. Born and E. Wolf, *Principles of Optics*, (Pergamon, Oxford, 1970).

[16]P. B. Johnson and R. W. Christy, Phys. Rev. B 6, 4370 (1972).

[17]H. Wolter, *Handbuch der Physik*, edited by S. Flugge (Springer, Berlin, 1956), Vol. 24, p. 461.

[18]There is a typographical error in Ref. 2. The numerator of Eq. (17) should contain k_0^3 instead of k_0^2.

[19]A. Otto (private communication).

[20]V. V. Bryksin, Yu. M. Gerbstein, and D. N. Mirlin, Phys. Status Solidi B 51, 901 (1972).

[21]This presents a problem in experimentally observing the SEW in anisotropic materials if one is attempting to locate the branches which terminate. This will be discussed in a future paper.

[22]N. Marschall, B. Fischer, and J. J. Queisser, Phys. Rev. Lett. 27, 95 (1971).

[23]W. E. Anderson, R. W. Alexander, Jr., and R. J. Bell, Phys. Rev. Lett. 27, 1057 (1971).

[24]I. I. Reshina, Uy. M. Gerbstein, and D. N. Mirlin, Fiz. Tverd. Tela 14, 1280—1282 (1972) [Sov. Phys.—Solid, State 14, 1104 (1972)].

[25]V. V. Bryksin, D. N. Mirlin, and I. I. Reshina, Solid State Commun. 11, 695 (1972).

[26]H. Y. Fan in *Optical Properties of III–V Compounds*, edited by R. K. Willardson and A. C. Beer (Academic, New York, 1967).

[27]J. Picht, Ann. Phys. (Leipzig) 3, 433 (1929).

[28]K. L. Kliewer and R. Fuchs [Phys. Rev. 144, 495 (1966)] have solved the radiative modes of an ionic slab with damping for ω complex and k complex but not the surface or nonradiative modes with damping.

[29]A. S. Barker, Jr., Phys. Rev. Lett. 28, 892 (1972).

[30]A. S. Barker, Jr., Surf. Sci. 34, 62 (1973).

[31]A. S. Barker, Jr., Phys. Rev. B 8, 5418 (1973).